



Gray, D. and Le Kernec, J. (2020) Scan Performance of Small Spherical Retro-Reflectors. In: 2019 International Radar Conference, Toulon, France, 23-27 Sept 2019, ISBN 9781728126609 (doi:[10.1109/RADAR41533.2019.171391](https://doi.org/10.1109/RADAR41533.2019.171391))

There may be differences between this version and the published version. You are advised to consult the publisher's version if you wish to cite from it.

<http://eprints.gla.ac.uk/184545/>

Deposited on: 18 April 2019

Enlighten – Research publications by members of the University of Glasgow
<http://eprints.gla.ac.uk>

Scan performance of small spherical retro-reflectors

D. Gray

Electrical Engineering

XJTLU

Suzhou, China

derek.gray@xjtlu.edu.cn

J. Le Kerneec

Electrical Engineering

Glasgow University

Glasgow, Scotland

julien.lekerneec@glasgow.ac.uk

Abstract—A number of historical small spherical lens retro-reflectors were simulated in a commercially available antenna simulator. This 1dBm² class retro-reflectors had radii of 2 free space wavelengths, allowing the use of a minimal number of layers to approximate the theoretical Luneburg profile. It was found that further simplification to a 2-layer lens or a single custom material lens were practical. In both cases, RCS of 1.5dBm² were achieved with 3dB scan ranges of 130°.

Keywords—component, formatting, style, styling, insert

I. INTRODUCTION

Passive retro-reflectors reflect the majority of incident energy back in the direction of the illuminator, without the need for an external power supply [1]. These retro-reflectors are used as beacons to mark the edges of aircraft runways, to augment small vessels by making a larger return, and for calibrating radar measurements to an absolute value.

For student radar projects, having low cost in-house manufactured calibration targets would be advantageous. In the past, metal spheres were used to provide absolute radar cross section (RCS) data for calibration, but have a relatively low backscatter as most of the incident energy is reflected in directions other than that of the illuminator. In contrast, a Luneburg lens fitted with a reflective cap reflects all of the incident energy in phase so the RCS is the same as that of a flat plate. A good description of the use of Luneburg lens retro-reflectors in the field for calibrating soil moisture measurements during a lengthy measurement campaign was given in [2].

Theoretically, a Luneburg lens is a sphere that has relative permittivity $\epsilon_r=2$ at the centre and a continuous decrease with radial position to $\epsilon_r=1$ at the sphere surface. As such, the Luneburg lens is a limiting case having surface $\epsilon_r=1$; non-Luneburg lenses having surface $\epsilon_r>1$ to be built from natural plastics can be designed using either closed form equations or full wave software. In either case, realising the continuous ϵ_r profile in a sphere is impossible, so the lens ϵ_r profile is discretised into a series of unique ϵ_r steps and the lens built from thin concentric spherical shells, Figure 1. However, from prior work on lens antennas for communications systems it is understood that single material homogeneous spherical lenses give adequate performance up to about 5 wavelength (λ_0) radius [3], obviating the need for the expensive concentric shell structure for Gain below 28dBi. For the 28dBi to 35dBi Gain range, a 2-layer cross-linked polystyrene (xPS) core with polyethylene (PE) outer layer lens has proven successful [4]. The only disadvantage of this type is the relatively high mass compared to Luneburg lenses due to the specific gravity of the natural plastics. The aim for this work is to test homogeneous and the 2-layer xPS-PE lenses as spherical retro-reflectors.

The angular arc of the metallic cap determines the angular range over which the lens gives a high value RCS. It

is normal practise to use a 140° metallic cap which gives a high RCS across about 120°, hence sets of 3 lenses been used to give full 360° coverage in the horizontal plane for marine buoys and light craft. A 140° metallic cap is illustrated in Figure 1, and was used in all simulations presented here.

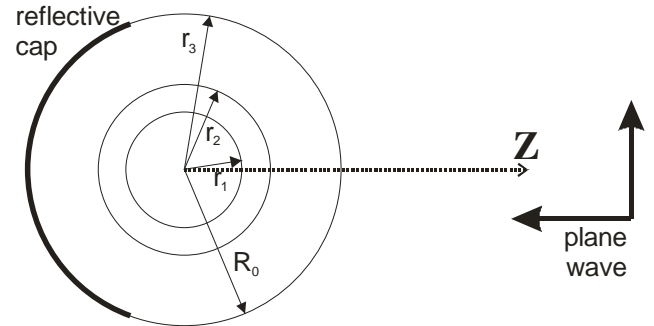


Fig. 1. Spherical lens topology simulated in FEKO™.

Here the commercially available Method of Moments antenna simulator FEKO™ using Higher Order Basis Function curvilinear elements was used to model the response to a linearly polarised plane wave of 2 historical 2 wavelength radius spherical retro-reflector lenses and some derivative designs. Material losses were not considered in the FEKO™ simulations. The centre frequency was 12GHz to be compatible with existing experimental equipment. The numerical simulation results were compared to the theoretical free space radar cross section of a metallic sphere was -11.1dBm² and for a spherical lens 0.9dBm².

II. OMNI-DIRECTIONAL REFLECTOR

As an alternative to a Luneburg lens with a reflective cap, a lens having total internal reflection was designed, built and tested [5]. The advantage of this lens was that it would give a constant RCS independent of illumination incident angle, not having a limited angular range dictated by a spherical cap. In stark contrast to the spherical lens designs mentioned above, this theoretical lens design had infinite ϵ_r at the sphere centre, with the permittivity falling away rapidly with increasing lens radius to $\epsilon_r=1$ at the lens surface, Figure 2. The ϵ_r profile was discretised into constant ϵ_r steps so that the lens could be built from concentric spherical shells of unique materials, as described above. The original structure built and tested had a small high ϵ_r ceramic core [5], which was simplified in the second version to a metallic sphere, Figure 2. The latter version was simulated here.

As the effect of the number of layers upon lens RCS was not discussed in [5], it was investigated here. The lens profile outside of the 4.8mm radius (0.0952R₀) metallic core was discretised in 4, 6, 8 and 10 equal ϵ_r steps here, Figure 2. These 4 lenses were illuminated by a linearly polarised plane wave coming from $\theta=0^\circ$ in FEKO™ and the RCS in

the principal and $\phi=45^\circ$ plane were noted. As the number of layers was increased, the $\theta=0^\circ$ RCS increased to an apparent asymptote equal to the RCS of an equal sized metallic sphere, Figure 3. This was an unexpectedly poor result.

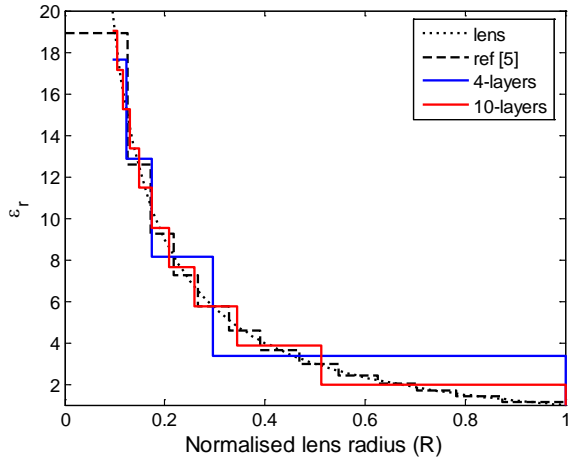


Fig. 2. Total internal reflection lens ϵ_r radial variation curve and discretised versions.

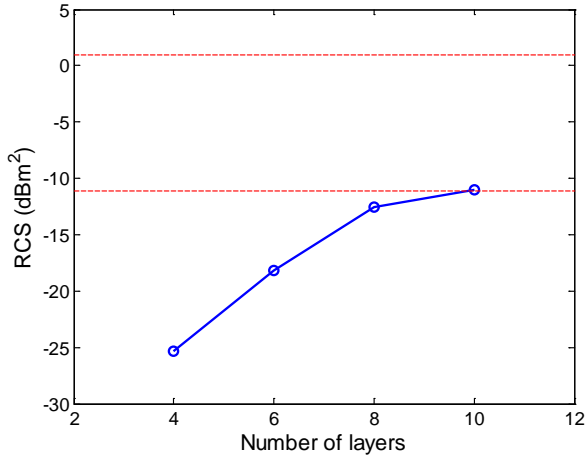


Fig. 3. Effect of number layers on total internal reflection lens $\theta=0^\circ$ RCS.

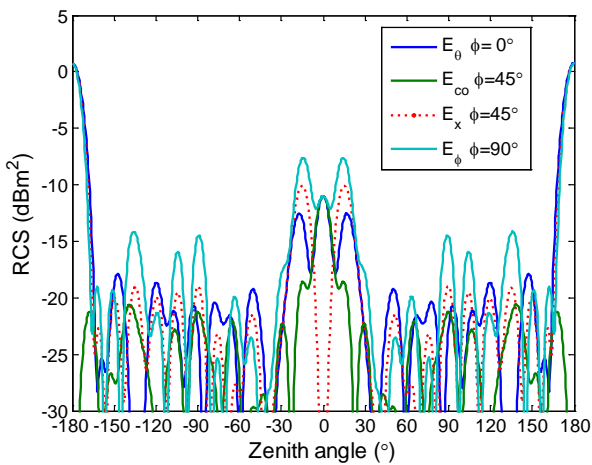


Fig. 4. Principal plane RCS patterns of 10-layer total internal reflection lens.

Examining the RCS patterns of the 10-layer implementation, it showed 3 major types of loss in the radiation pattern around the $\theta=0^\circ$ direction that led to the poor RCS result, Figure 4. In the E-plane ($\phi=0^\circ$), the first side lobes were of almost equal amplitude as the mainlobe. In the $\phi=45^\circ$ plane, the cross-polarised radiation component had a higher amplitude than the co-polarised component. In the H-plane ($\phi=90^\circ$), the mainlobe was split by a null in the $\theta=0^\circ$ direction. Overall, this lens type, as a circular aperture, had poor illumination and lost a significant amount of energy into the cross-polarised component in the $\phi=45^\circ$ plane. A metallic sphere would be a lower cost option for an equal RCS response.

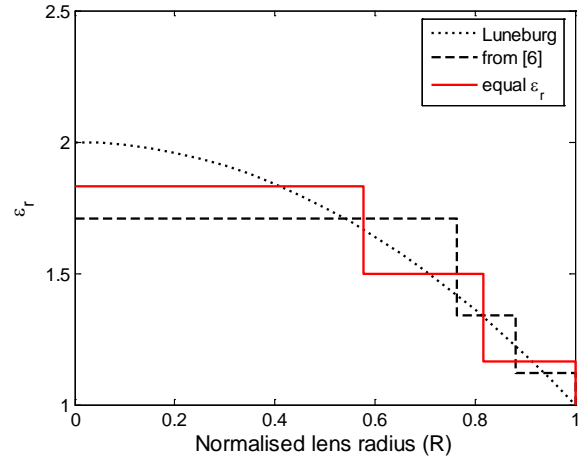


Fig. 5. Historical and equal ϵ_r step 3-layer simplified Luneburg lens designs.

III. SMALL RADII LUNEBURG LENSES

Simplifying and thus reducing the manufacturing cost of Luneburg lenses by using a large homogeneous core was expounded in [6]. For the relatively small $2\lambda_0$ radius class of lens considered here, a core of $\epsilon_r=1.71$ of radius $R=0.764R_0$ was suggested, with 2 thin outer layers, Figure 5. Superficially, the design does not center on the Luneburg curve and appears to be biased toward higher ϵ_r . For comparison, the Luneburg curve was discretized into 3 equal ϵ_r steps. Both 3-layer Luneburg lenses were simulated in FEKOTM with a 140° PEC cap.

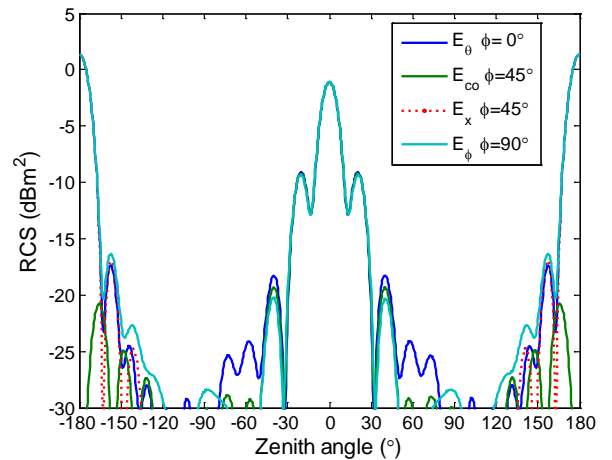


Fig. 6. Principal plane RCS patterns of 3-layer Luneburg reflector from [6].

In contrast to the total internal reflection lens, the 3-layer Luneburg lens produced a distinct and fully rotationally symmetric main beam consisting of a mainlobe and first sidelobes, Figure 6. Additionally, the $\phi=45^\circ$ plane cross-polarised component was more than -30dB below the mainlobe peak. The forward ($\theta=0^\circ$) RCS was -1.1dBm^2 . The equal ϵ_r step 3-layer Luneburg gave a forward RCS of 0.63dBm^2 , which is closer to the theoretical RCS value of 0.94dBm^2 for a $2\lambda_0$ radius spherical lens. The latter gave 1.7dB better performance due to lower relative first sidelobe level.

IV. 2-LAYER THORNTON LENS

As described in the Introduction, the 2-layer xPS-PE lens was extensively evaluated as a medium gain antenna for communications systems. As a 2-layer spherical structure it is preferable to a 3-layer structure. Here a $2\lambda_0$ radius version was simulated in FEKOTM, with the xPS $\epsilon_r=2.53$ core extending from the sphere center to $R=0.47R_0$, and the outer PE layer had $\epsilon_r=2.3$. The forward RCS was 1.5dBm^2 , exceeding the theoretical RCS value of 0.94dBm^2 . This good result is due to the first sidelobe level been 16.5dB below the $\theta=0^\circ$ peak, which was close to 17dB expected of a uniformly illuminated circular aperture.

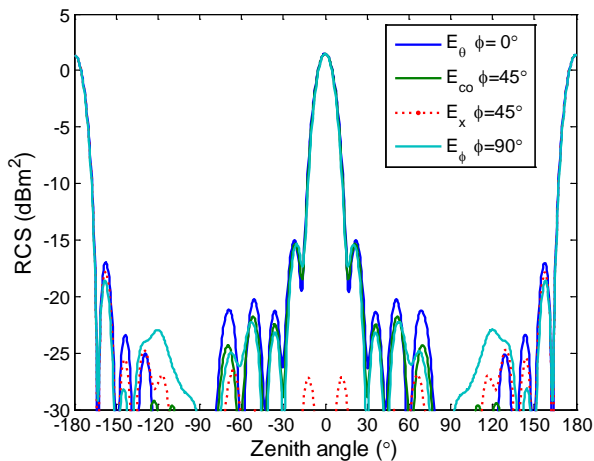


Fig. 7. Principal plane RCS patterns of 2-layer xPS-PE lens.

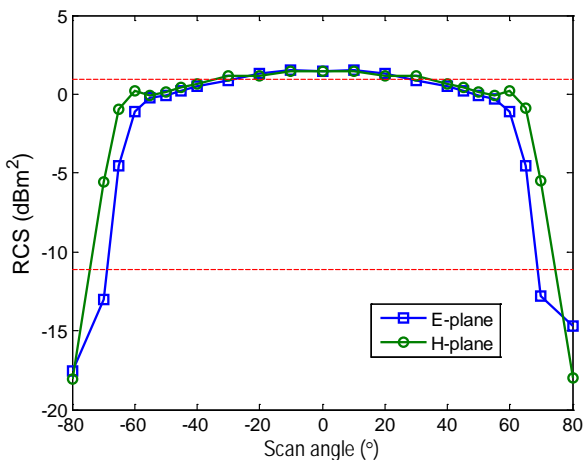


Fig. 8. Principal plane scan performance of 2-layer lens.

To check the practicality of the 2-layer xPS-PE lens, it was rotated $\pm 80^\circ$ in both the E-plane and the H-plane. As expected from prior work on Luneburg lenses, the scan range was limited by the 140° metallic cap, Figure 8. The E-plane 3dB beamwidth was 123° and the H-plane 3dB beamwidth was 134° , which are satisfactory results.

If manufactured from xPS and PE, the $2\lambda_0$ radius lens weight will be approximately 520grams for 12GHz. This weight is prohibitively high for a small platform like a quadrotor, but acceptable for man-portable use and larger platforms such as fishing boats.

V. HOMOGENEOUS LENSES

As a further simplification, a simple homogeneous sphere with 140° metallic cap was simulated in FEKOTM. The ϵ_r was varied from 1.7 to 3.5, Figure 9. Above $\epsilon_r=2.60$, the forward RCS was comparable to or exceeded the theoretical RCS value of 0.94dBm^2 . The peak RCS value was 2.7dBm^2 for $\epsilon_r=2.90$. This result is peculiar to the relatively small $2\lambda_0$ radius and is not expected to be repeated at larger radii where the phase error in a homogeneous lens will become significant [6].

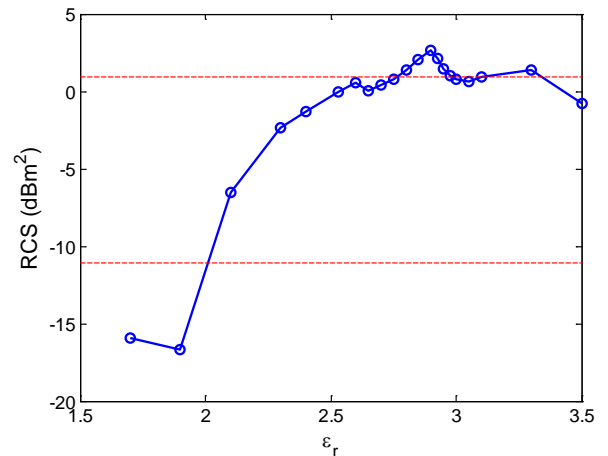


Fig. 9. Effect of ϵ_r on RCS of $2\lambda_0$ radius homogeneous sphere.

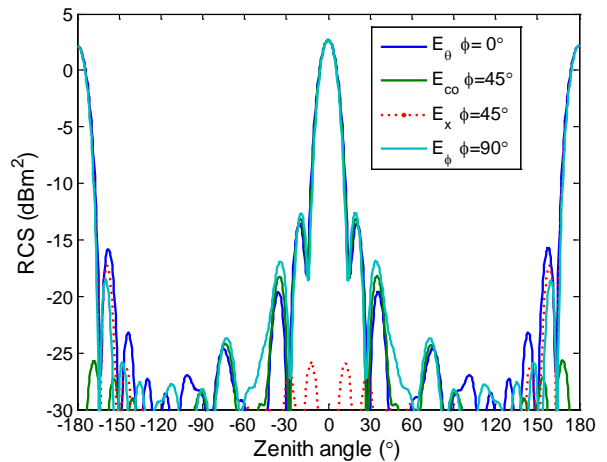


Fig. 10. Principal plane RCS patterns of $\epsilon_r=2.90$ homogeneous lens.

Similar to the 2-layer xPS-PE lens, a good forward RCS value was given by the $\epsilon_r=2.90$ lens as it produced a good rotationally symmetric main beam having first sidelobe level

15.3dB below the $\theta=0^\circ$ peak, and the $\phi=45^\circ$ plane cross-polarised component was about -30dB below peak.

The scan performance of the 3-layer Luneburg lenses and the $\epsilon_r=2.90$ homogeneous lens will be given in the full paper.

ACKNOWLEDGMENT

This work was started at NICT Satellite Communications Group under the direction of Dr. R. Suzuki during the 2009/10 fiscal year.

REFERENCES

[1] D. Bird, "Design and manufacture of a low-profile radar retro-reflector," presented at the *RTO SCI Symposium on Sensors and*

Sensor Denial by Camouflage, Concealment and Deception, Brussels, Belgium, 19-20 April 2004, RTO-MP-SCI-145.

- [2] F.T. Ulaby, "Measurement of soil moisture content," *CRES Technical Report 177-35*, April 1973.
- [3] D. Gray, J. Thornton, H. Tsuji & Y. Fujino, "Scalar feeds for 8 wavelength diameter homogeneous lenses," *IEEE Int. Ant. and Prop. Symp.*, North Charleston, June 2009.
- [4] J. Thornton, "Wide-scanning multi-layer hemisphere lens antenna for Ka band", *IEE Proc.-Microw. Antennas Propag.*, Vol. 153, No. 6, December 2006.
- [5] N. Ochai, "Omnidirectional dielectric lens reflector," *United States patent 3,550,147*, granted Dec. 22, 1970.
- [6] N. Ochiai, "Shell-type luneberg lens," *United States patent 3,465,362*, granted Sep. 2, 1969.